Numerical study for the two-beam instability due to ions in electron-storage rings

Kazuhito Ohmi
KEK, National Laboratory for High Energy Physics, Oho, Tsukuba, Ibaraki 305, Japan
(Received 13 January 1997)

We discuss the two-beam instability which is caused by interactions between ions and the electron beam in electron storage rings. Motion of beam and ions trapped in the beam potential was studied by using a simulation method based on a rigid Gaussian beam model. We consider two types of the two beam instability depending on the trapped time. One is the so-called ion trapping instability, in which ions are accumulated every revolution. The growth of the coupled bunch mode, which was obtained by simulations, was consistent with experiments in the KEK-photon factory. The other is the fast ion instability, in which ions are trapped during only the passage of a single series of bunches (bunch train). Simulations gave the growth of the couple bunch mode for the KEK-B factory. [S1063-651X(97)00306-1]

PACS number(s): 29.20.Dh, 29.27.Bd, 41.75.Ht

I. INTRODUCTION

The electron beam in a storage ring creates ions by ionizing the residual gas in the beam chamber. In a storage ring filled by electron bunches with a narrow spacing, ions with a mass larger than a critical value are trapped by the attractive force of the electron beam. The trapped ions, which oscillate in the beam potential, cause the two-beam instability due to a coupling to the coherent motion of the beam. We have observed a coupled bunch instability caused by the two-beam effect.

We discuss here the dynamics of two-beam instability using a computer simulation. The simulation method, which is based on the weak-strong model, was discussed in the case of beam-beam interactions in Ref. [1]. This method is very useful for studying the two-beam instability due to beam-ion interactions. In this method, a weak beam of ions is expressed by macroparticles, while only the barycenter motion of the strong beam is taken into consideration.

In considering the simulation, the beam-beam and beam-ion interactions are very similar. The differences between them can be summarized as follows. In the general case of beam-beam interactions, a bunch interacts with only another bunch, and both bunches move at the speed of light. However, the ions move nonrelativistically and interact with all of the bunches. The number of ions increases in every passing bunch. Though a space-charge force between the ions exists because of a nonrelativistic effect, since the number of ions, which causes the two-beam instability, is generally very small, as shown later, we can neglect it.

We now consider the transverse motion of electrons and ions. We neglect the effect of the magnetic field. The equations of motion for electrons and ions are expressed as

$$\frac{d^2\mathbf{x}_{e,a}}{ds^2}+K(s)\mathbf{x}_{e,a}=\frac{2r_e}{\gamma}\sum_{j=1}^{N_i}\mathbf{F}(\mathbf{x}_{e,a}-\mathbf{x}_{i,j}), \tag{1}$$

$$\frac{d^2\mathbf{x}_{i,j}}{dt^2}=\frac{2r_ec^2}{M_i/m_e}\sum_{a=1}^{N_e}\mathbf{F}(\mathbf{x}_{i,j}-\mathbf{x}_{e,a}), \tag{2}$$

where suffices i and e denote the ion and electron, respectively. M_i and m_e are masses, and N_i and N_e are the number of each. γ and r_e are the Lorentz factor of the beam and the classical electron radius, respectively. $\mathbf{F}(\mathbf{x})$ is the Coulomb force in two dimensional space,

$$\mathbf{F}(\mathbf{x})=-\frac{\mathbf{x}}{|\mathbf{x}|^2}\delta(s). \tag{3}$$

These consist of N_e+N_i differential equations, where each electron couples to the motion of all ions, and each ion couples to the motion of all electrons.

We now consider the species of ions. The residual gas component in the vacuum chamber are mostly CO and H_2. A typical spectrum in the photon factory (PF) [2] consisted of 48% for CO and 41% for H_2. The ionization cross sections are 1.8×10^{-22} and 0.3×10^{-22} m^2 for our beam energy of 2.5 GeV. The cross section of CO is about six times higher than that of H_2. We assume that CO plays a dominant role in the two-beam instability, and neglect other species of ions hereafter.

The two-beam instability is a collective effect obtained by solving Eqs. (1) and (2). This was originally discussed in plasma physics. In accelerator physics, it was considered for the first time in the case of the electron-trapping instability in a proton ring [3,4]. Concerning ion-beam interactions, the two-beam instability has been studied in most electron storage rings operated in multibunch mode. The instability has been discussed based on linear theory [3]. Linear theory is reviewed and discussed with an example of the KEK-photon factory (PF) and the KEK-B Factory (KEKB) in Sec. II. In Sec. III, our simulation method based on the weak-strong model is explained. This method permits the study of the two-beam instability beyond linear theory and from a dynamic aspect. The results of a simulation for PF (the ion-trapping instability) and KEKB (the fast-ion instability) are discussed Secs. IV and V.

II. LINEAR THEORY

The linear theory presented by Keil and Zotter is reviewed here. The following approximations are assumed in the theory.

The transverse motions of beam and ions are expressed only by their barycenters.

The coasting-beam approximation is used; that is, the beam has no longitudinal structure, and is specified by its transverse barycenter at longitudinal position z from a reference bunch and time $s=ct+z$.

The beam size can be treated as a constant along the ring; that is, the β function is assumed to be a constant.

The beam and ions are distributed according to a Gaussian with identical sizes in the transverse plane.

The beam-ion force is assumed to depend linearly on the distance between the barycenters.

With these assumptions, the equations of motion for the beam and ion are expressed as follows:

$$\frac{D^2\overline{\mathbf{x}_e}}{Ds^2}+\left(\frac{\omega_\beta}{c}\right)^2\overline{\mathbf{x}_e}=\frac{2n_i r_e}{\gamma}\mathbf{F}_L(\overline{\mathbf{x}_e}-\overline{\mathbf{x}_i}), \tag{4}$$

$$\frac{d^2\overline{\mathbf{x}_i}}{dt^2}=\frac{2n_e r_e c^2}{M_i/m_e}\mathbf{F}_L(\overline{\mathbf{x}_i}-\overline{\mathbf{x}_e}), \tag{5}$$

where

$$F_{L,y}(\mathbf{x})+iF_{L,x}(\mathbf{x})=-\frac{1}{\sigma_x+\sigma_y}\left(\frac{y}{\sigma_y}+i\frac{x}{\sigma_x}\right). \tag{6}$$

Here, n_e and n_i are the number of electrons and ions in a unit length, and ω_β is the betatron frequency. The differentiation with respect to s is expressed by

$$\frac{D}{Ds}=\frac{\partial}{\partial s}+\frac{\partial}{\partial z}. \tag{7}$$

Here, we try to obtain a solution with the following form:

$$\mathbf{x}(s,z)=\boldsymbol{\xi}\exp\left[i\left(\frac{2\pi mz}{L}-\frac{\Omega s}{c}\right)\right], \tag{8}$$

where m is an integer. We obtain a fourth-degree equation in Ω,

$$(\Omega^2-\omega_i^2)[(\Omega-m\omega_0)^2-\omega_\beta^2-\omega_e^2]=\omega_e^2\omega_i^2. \tag{9}$$

Here ω_i and ω_e are the frequency of the ion and betatron frequency shift ($=2\omega_\beta\delta\omega_\beta$) of the beam, respectively, and are given by

$$\omega_i^2=\frac{2n_e r_e c^2}{M_i/m_e}\frac{1}{\sigma_y(\sigma_x+\sigma_y)},\quad \omega_e^2=\frac{2n_i r_e c^2}{\gamma}\frac{1}{\sigma_y(\sigma_x+\sigma_y)}. \tag{10}$$

The two-beam instability occurs when the frequency (Ω) has an imaginary part. We investigate the case where the frequencies of the ions (ω_i) and beam ($\omega_\beta-m\omega_0$) in the experimental frame are close to each other, because the two-beam instability is the result of a coupling resonance between the two oscillators. We obtain the threshold and growth rate as

$$\omega_{e,th}=\frac{(m\omega_0-\omega_i)^2-\omega_\beta^2}{2\sqrt{\omega_i(m\omega_0-\omega_i)}}\quad \mathrm{Im}\left(\frac{\Omega}{\omega_0}\right)=\frac{\omega_e}{2\omega_0}\left(\frac{\omega_i}{m\omega_0-\omega_i}\right)^{1/2}. \tag{11}$$

TABLE I. Parameters of PF and KEKB.

	PF	KEKB
Circumference(m)	186	3016
Revolution frequency($\omega_0/2\pi$)	1.6×10^6	10^5
Energy(GeV)	2.5	8
Current (A)	0.4	1.1
Vertical tune (ν_y)	3.305	43.08
Harmonic number	312	5120
Emittances ε_x(nm), ε_y(nm)	130, 1.5	18, 0.36
Transverse radiation damping rate	8×10^{-5}	1.2×10^{-4}

From $\omega_{e,th}$, we obtain $n_{i,th}$ using Eq. (11).

In linear accelerators and in the bunch train of circular accelerators, a threshold does not exist in the ion-beam system alone because m is nearly continuous. The actual threshold is determined by a comparison with other damping effects.

It is well known that these equations show a very low threshold and a very high growth rate in recently developed accelerators. We discuss them in the cases of KEK-PF and KEKB. The parameters are given in Table I. Examples of the results obtained by the linear theory are shown in Table II. In Table II, threshold is given with the neutralization factor ($\eta=n_i/n_e$). These high growth rates are surprising. However, since we did not consider the ion increase due to production, we should not immediately believe the growth rate.

When the threshold is extremely low, as shown in the KEKB case, we should consider the two-beam instability due to transient ions, the so-called fast-ion instability. If we use a production cross section of $\sigma_{\mathrm{CO}}=2.0\times10^{-22}$ m^2 for our beam energy of 8 GeV and a partial pressure of $P_{\mathrm{CO}}=10^{-9}$ Torr, a bunch including $N_e=1.4\times10^{10}$ ($n_e=2.1\times10^{10}$ m^{-1}) electrons produces about 100 ions per meter. If 1000 bunches pass, the neutralization factor becomes $\eta=5\times10^{-6}$, which already exceeds the threshold. This suggests the possibility of a fast-ion instability in KEKB.

Equation (9) has a singularity at $\omega_i=\pm(m\omega_0-\omega_\beta)$. In practical cases, the ion frequency (ω_i) has a spread due to the nonlinearity of the beam-ion force and the beam size from the variation of the $\beta(s)$ function. The linear theory has been extended to include the frequency spread by Refs. [5–7]. A linear theory including an ion increase for linear accelerators is given in Ref. [6].

III. BEYOND LINEAR THEORY

We now restart our discussion from Eqs. (1) and (2). The weak-strong model is being proposed to study the two-beam instability. In this model, the transverse distribution of the

TABLE II. Results obtained by linear theory.

	I (A)	ω_i/ω_0	η_{th}	$\mathrm{Im}(\Omega/\omega_0)$
PF	0.04	0.740	0.0015	0.022
	0.4	2.339	0.003	0.169
KEKB	1.1	139.535	8.1×10^{-7}	0.192

beam is assumed to be a rigid Gaussian, where the deviation is determined by the emittance and β function; that is, deformations of the bunch due to ions are neglected. The effects of the bunch length and the synchrotron motion are not considered. The beam is not characterized by each electron, but by a series of bunches with a rigid Gaussian distribution. By averaging Eq. (1), we take into account only the first-order moment. Ions are treated exactly, except for neglecting their longitudinal motion. The equation of motion for a bunch and ions are expressed as

$$\frac{d^2\overline{\mathbf{x}_e}}{ds^2}+K(s)\overline{\mathbf{x}_e}=\frac{2r_e}{\gamma}\sum_{j=1}^{N_i}\mathbf{F}_G(\overline{\mathbf{x}_e}-\mathbf{x}_{i,j};\boldsymbol{\sigma}(s)), \tag{12}$$

$$\frac{d^2\mathbf{x}_{i,j}}{dt^2}=\frac{2N_e r_e c^2}{M_i/m_e}\mathbf{F}_G(\mathbf{x}_{i,j}-\overline{\mathbf{x}_e};\boldsymbol{\sigma}(s)), \tag{13}$$

where $\mathbf{F}_G$ is expressed by the Bassetti-Erskine formula [8],

$$F_{G,y}(\mathbf{x})+iF_{G,x}(\mathbf{x})=\left(\frac{\pi}{2(\sigma_x^2-\sigma_y^2)}\right)^{1/2}\left[w\left(\frac{x+iy}{\sqrt{2(\sigma_x^2-\sigma_y^2)}}\right)-\exp\left(-\frac{x^2}{2\sigma_x^2}-\frac{y^2}{2\sigma_y^2}\right)w\left(\frac{\frac{\sigma_y}{\sigma_x}x+i\frac{\sigma_x}{\sigma_y}y}{\sqrt{2(\sigma_x^2-\sigma_y^2)}}\right)\right]\delta(s). \tag{14}$$

Here N_e is the number of particles in a bunch. These equations of motion, Eqs. (12) and (13), can be solved by an approximation in which ions are represented by macroparticles, and the barycenter motion of every bunch are obtained. If a coherent (correlated) bunches mode grows, a coupled-bunch instability is caused. In this case, we conjecture that ions also move coherently. It can be ascertained by calculating the moments of the macroions.

The incoherent features of ions can be obtained by our simulation, while that of the electron beam, such as emittance growth, cannot be computed. If the tune spread due to the ion distribution is large, the coherent motion may be smeared and the beam size enlarged, i.e., Landau damping occurs. The smear is expressed as

$$\delta\omega_\beta=\frac{\omega_e^2}{2\omega_\beta}=\frac{n_i r_e c^2}{\gamma\omega_\beta}\frac{1}{\sigma_y(\sigma_x+\sigma_y)}. \tag{15}$$

The problem is which is the larger, the growth rate of the two-beam instability or the damping rate due to the smear. In our examples, the linear theory shows that the growth rate is larger. Using PF parameters, I=40 mA and $\eta=0.01$, as an example, the growth rate is 0.045, while the damping rate (tune spread) is 0.009. If the Landau damping rate becomes important, this simulation will overestimate the growth of the instability.

The original differential equations of Eqs. (1) and (2) can be solved with macroparticles for both electrons and ions (strong-strong simulations). Strong-strong simulations have been recently performed for the fast-ion instability [6,9]. In strong-strong simulations, the motion of many macroelectrons and ions are tracked by using a lot of computer resources. Strong-strong simulations include the smear effect.

In the weak-strong simulation, the overestimation of the growth results in a trade off between accuracy and a shorter CPU time. The simulations should be performed while paying attention to the Landau damping rate. We discuss this problem again concerning the applications.

We now comment on the smear of the ion motion. The smear of ions, which is just ω_i, is much faster than that of the beam in the usual case. In terms of a beam-beam interaction, one says that the tune shift of ions is larger than that of the beam in the ion-beam interactions. The smear of the beam may be reduced by the faster smear of ions. This weak-strong model completely involves the smear of ions.

The ion-trapping and the fast-ion instability are discussed by using this simulation in Sec. IV and in Sec. V, respectively. Both instabilities are caused by the same mechanism. The difference is how long the ions are trapped in the beam potential. One instability is caused by ions which are accumulated turn by turn, and the other by the passage of a bunch train.

IV. APPLICATION TO THE ION TRAPPING

We discuss the two-beam instability due to ion-trapping using the PF as an example. To survey features of the instability, some (fixed) amount of macroions were put along an unperturbed beam orbit, and the motion of the ions and bunches were investigated. The ring was represented by four ionization points with different values of the β function. It was checked that the results did not depend on the number of ionization points. A thousand macroions were put at each point. All of the bunches were set with zero displacement. We calculated the kick felt by ions using Eq. (13). The force which the beam feels was obtained by summing over the ions. After being kicked, the beam is advanced to the next ionization point. The resulting system is metastable. The actual instability is caused by the statistical fluctuation of the barycenter position of the macroions. We discuss only the vertical motion of ions and beam, because simulations show that the coherent mode of the horizontal motion is much less than the vertical one.

The time evolution of the amplitude of the bunches which pass through an ionization point in a ring is shown in Fig. 1. The amplitude was obtained at a position with $\beta_y=28.3$ m: $\sigma_y=0.19$ mm. We use the parameters of $I=40$ mA for PF. The ion frequency (ω_i) is $0.74\times\omega_0$ from Table II. It is close to the coherent frequency of the beam with $m=4$, i.e., $m-\nu_y\sim 4-3.3=0.7$. We found that the phase advance of the coupled-bunch motion was about $0.7\times 2\pi$ rad in each revolution. The barycenter and size of the ion distribution of the ionization point are also plotted in Fig. 1. The barycenter of the ions also oscillates with the same frequency as the bunches. The coupled-bunch mode means that the two-beam instability is caused by a resonance between the frequencies of the beam coherent motion of $m=4$ and the ions. The ion size is about $1/\sqrt{2}$ of the beam size between 2–8 revolutions. The size reduction comes from the smear of ions. It is interesting that the ion size also becomes larger along with the growth of the dipole amplitude. The coherent motion of the

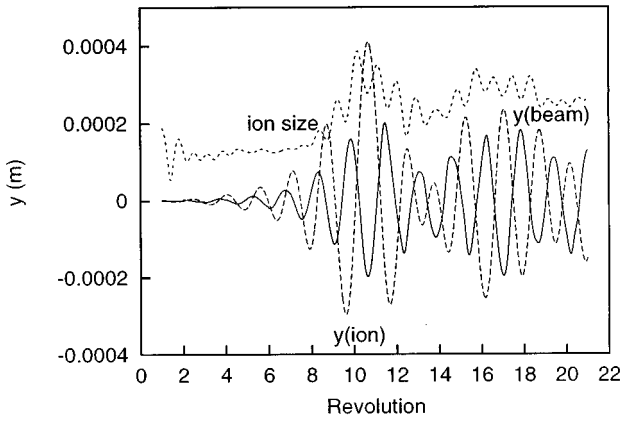

FIG. 1. Coupled-bunch pattern due to ion-trapping in KEK-PF. The neutralization factor is 1%. Vertical coherent amplitudes of bunches and ions, and size of ions are plotted.

ions is accompanied by their blowup coming from the rapid smear due to the beam force.

The same calculations were then performed for various values of the neutralization factor. Figure 2 shows the time evolution of the maximum amplitudes of the bunches and ion distribution sizes for each revolution, respectively. The figures shows that the ion size and the beam amplitude grow at

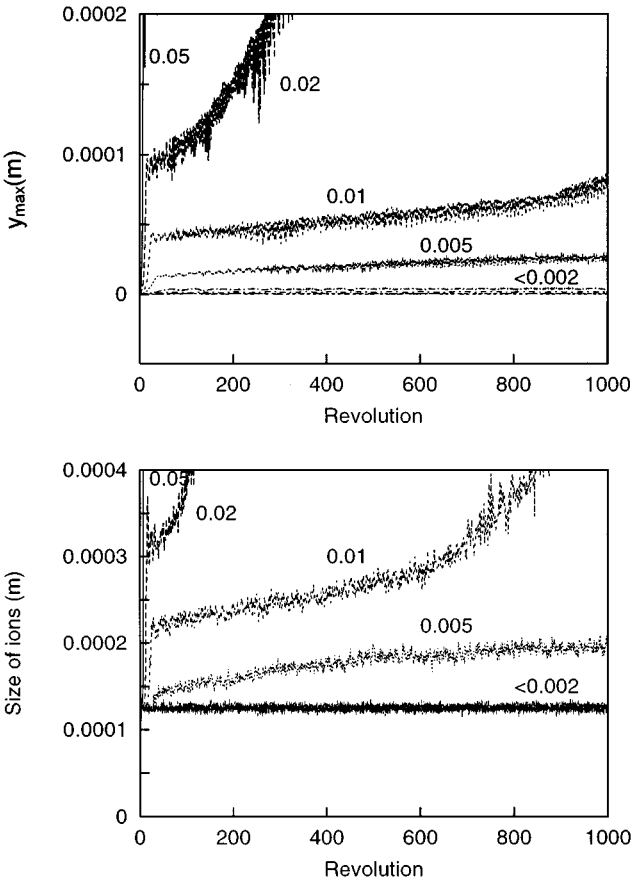

FIG. 2. Maximum vertical amplitude of the bunch coherent motion and vertical size of the ions. The amplitude and size are plotted at every revolution for various neutralization factors as written on the figure.

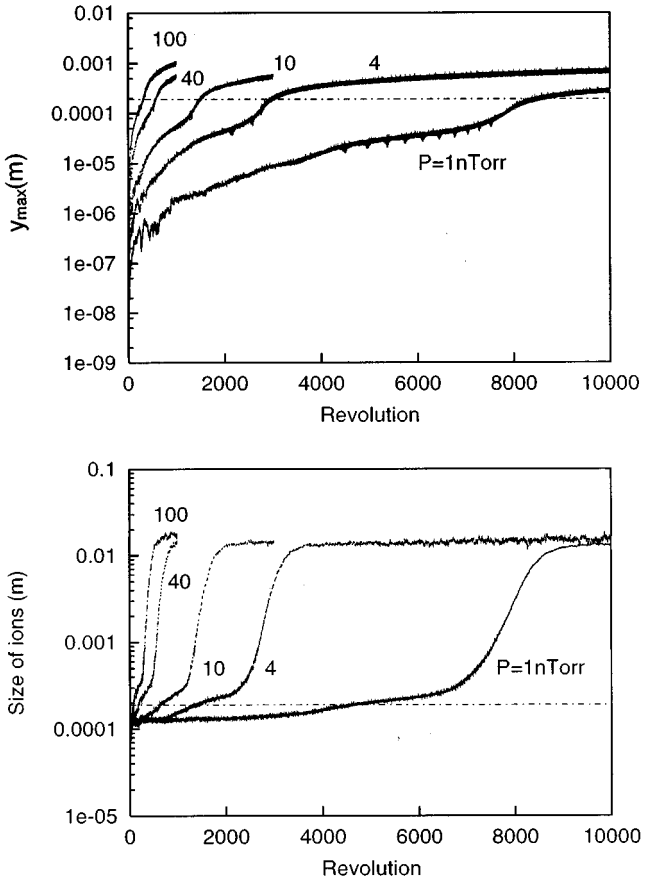

FIG. 3. Maximum amplitude of the bunches and size of ions. The amplitude and size are plotted at every revolution for various vacuum pressures as written on the figure.

$\eta \geqslant 0.005$. We may be able to say that the threshold for the neutralization factor is less than 0.005.

In an actual accelerator, since ions are continuously supplied, the time evolution of the instability depends on the creation rate of ions, which is related to the vacuum pressure. We took into consideration the ion increase in the simulation: macroions are produced by bunches in proportion to the vacuum pressure, and the bunches feel a force due to the ions, which increases at every bunch passage.

As previously done, the ring was represented by four ionization points. In every passing of the bunches through an ionization point, new macroions were generated at the transverse position of the bunch with a Gaussian distribution. Though 1 or 10 macro-ions were generated for every revolution time, results were not affected by the number. Figure 3 shows the growth of the dipole amplitude and the ion distribution size for $P_{CO} = 10^{-7}$, 4×10^{-8}, 10^{-8}, 4×10^{-9}, and 10^{-9} Torr. In these parameters, the neutralization factor increases by 10^{-4} for $P_{CO}=10^{-7}$ Torr every revolution time. The maximum amplitude exceeds $\sigma_y \equiv 0.19$ mm at a neutralization factor of ~ 0.01. Figure 3(b) shows that the ion size increases rapidly in spite of the small beam amplitude ($\ll \sigma_y$). Though the figure shows a saturation at around a few cm, it results from the boundary (5 cm) of the vacuum chamber. Figure 4 shows the number of accumulated ions in the vacuum chamber. The ions are thrown away in spite of the relatively small amplitude of the beam ($\sim \sigma_y$).

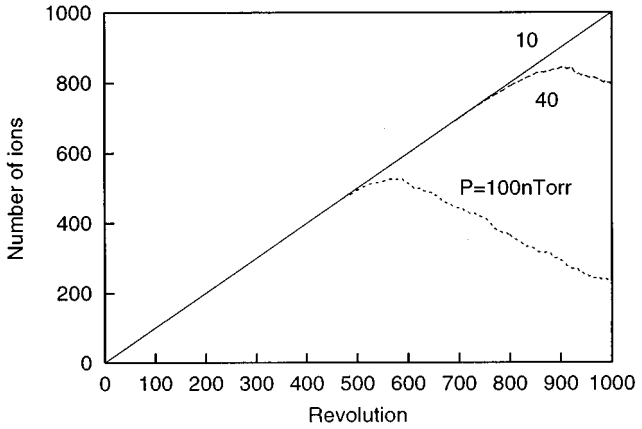

FIG. 4. Number of ions in a vacuum chamber. The vertical axis is normalized by the number of ions which are created in one revolution.

Figure 5 shows the growth time for various stored currents and vacuum pressures. The same calculations were performed for a stored current (I) of 400 mA; the results are plotted in the figure. PF has been operated with $P_{\mathrm{CO}}=10^{-9}$ Torr or less. The figure shows that the growth time is $\sim$1200 and $\sim$200 turns for stored currents of 40 mA and 400 mA, respectively, at the pressure. The two-beam instability due to ion trapping has been observed in PF [2]; its threshold was about 30–50 mA [10]. The instability has been controlled by exciting octupole magnets, which caused a Landau damping of several hundreds to $\sim$1000 turn near to the threshold. These results seem to be consistent with the experiments.

We now consider the smear of the beam due to the distribution of ions. This simulation did not include the smear directly because we used the rigid bunch model. However, we obtain the smear from the ion distribution by Eq. (15), where $\sigma_{x,y}$ was calculated by averaging the macroions. Figure 6 shows the tune spread. Since the smear is proportional to the square of the beam amplitude, the coherent motion is not smeared at small amplitude. On the other hand, for amplitudes larger than σ_y, since the ion distribution becomes broad, the smear becomes weak. In this regime, ions are diffused by the beam, and are eventually thrown out of the

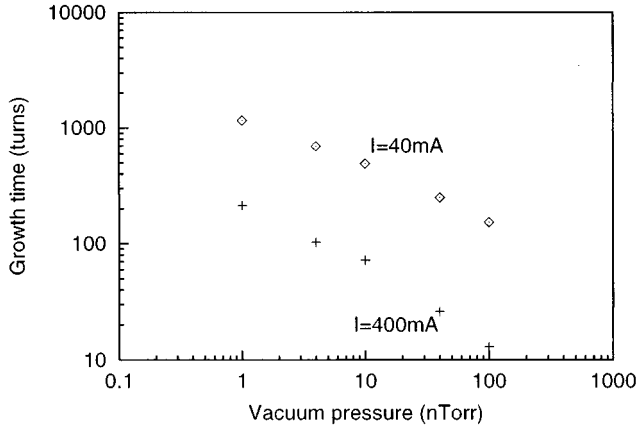

FIG. 5. Relation between growth time and vacuum pressure.

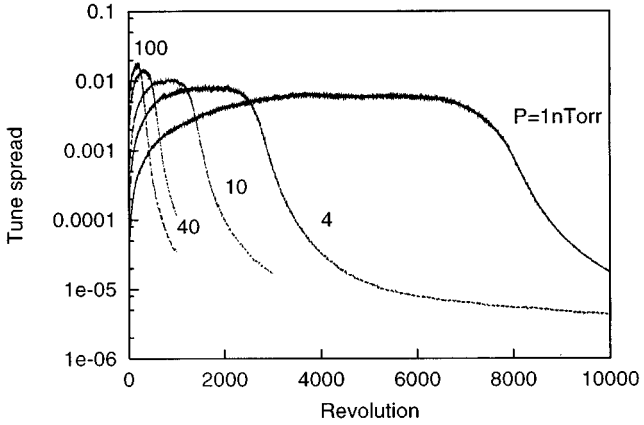

FIG. 6. Spread of the vertical tune due to the trapped-ion distribution.

chamber as shown in Figs. 3 and 4. This explains the pulsation phenomena observed at PF [2]. In the experiment, the number of trapped ions, which is measured with the bremsstrahlung of the beam, correlates to the pulsation of the instability. The experiment showed that the number of ions decreased rapidly when amplitude growth was caused by the two-beam instability, and increased again after the reduction of the growth.

V. APPLICATION TO THE FAST-ION INSTABILITY

In low-emittance high-intensity storage rings, the growth rate of the two-beam instability is very high. It is possible to cause an instability by ions which are produced and trapped in only one revolution, as mentioned in Sec. II. It is called the fast-ion instability [6]. We can simulate it in the same way.

We consider bunch trains in a ring. By putting a sufficient gap between the trains, the ions which are trapped during a passing bunch train are cleared after its passage. Thus the first bunch of a train does not face ions, while following bunches feel ions produced by the previous bunches in the train. The ions and bunches of the tail cause the two-beam instability.

The simulation results of KEKB are presented here. The train length is assumed to be 500. Four ionization points were chosen in the ring, as was done in the case of trapping. Macroions were created with a Gaussian distribution at the transverse position of the passing bunch at the ionization points. The number of macroions was ten for passing a bunch at a point. Results were the same when five macroions were used. Figure 7 shows the bunch pattern which is observed at the position of the ring. The ion's frequency is $140\times\omega_0\sim37\times\omega_{RF}$ as shown in Table II. The figure shows the induced coherent-mode oscillation whose frequency is equal to the ion's frequency.

Figure 8 shows the time evolution of the growth of the dipole amplitude of the bunches, where the amplitude is half of the Courant-Snyder invariant $[J_y\equiv(\gamma_y y^2+2\alpha_y yy'+\beta_y y'^2)/2]$. The growth times were 10 and 100 turns for vacuum pressures of 10^{-8} and 10^{-9} Torr, respectively, at a vertical amplitude of $0.5\sigma_y$. The growth becomes slow at an amplitude of about σ_y. The growth reduction seems to result

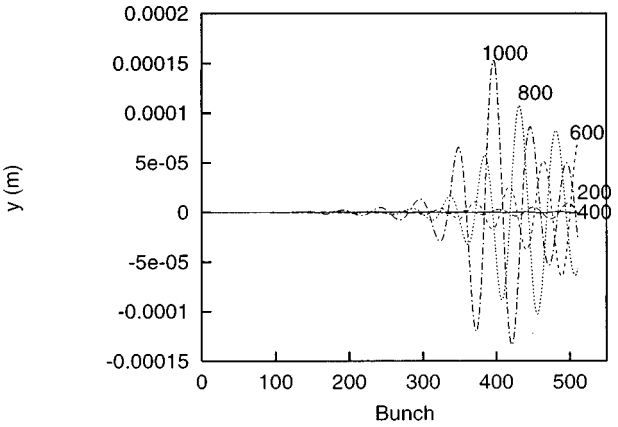

FIG. 7. Coupled-bunch pattern due to the fast-ion instability. The vacuum pressure is assumed to be 1 nTorr. Bunch patterns at the 200th, 400th, 600th, 800th, and 1000th revolution are drawn.

from the ion distribution size which is about $1/\sqrt{2}$ of beam's one. These were consistent with those obtained by the strong-strong simulation [9]. We have considered a feedback system to cure the instability in KEKB. The damping rate of the feedback has been designed to be 100 turns (1 ms). The length of the bunch train for which the feedback can cure was 500 for $P_{\mathrm{CO}}=10^{-9}$ Torr and was 100 for $P_{\mathrm{CO}}=10^{-8}$ Torr.

We investigated the effect of residual ions which are not

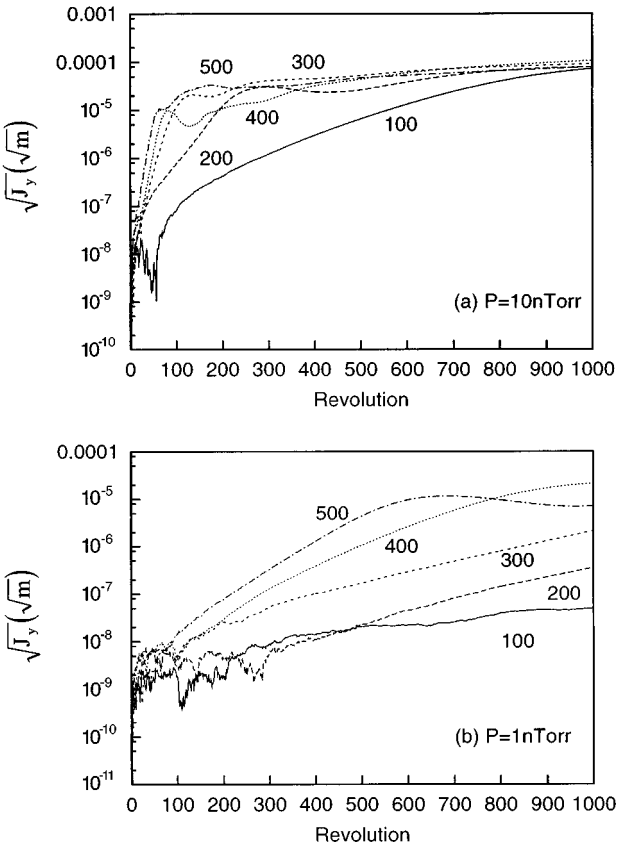

FIG. 8. Time evolution of the amplitude of selected bunches. Amplitudes of the 100th, 200th, 300th, 400th, and 500th bunches are plotted for $P=10^{-8}$ Torr (a) and $P=10^{-9}$ Torr (b).

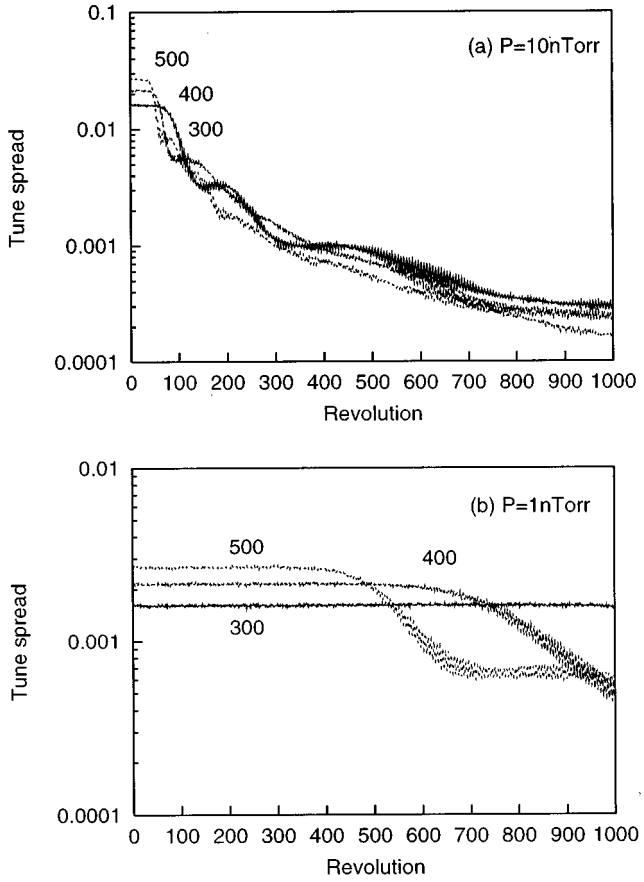

FIG. 9. Spread of the vertical tune due to the ion distribution. Tune spreads of the 300th, 400th, and 500th bunches are plotted for $P=10^{-8}$ Torr (a) and $P=10^{-9}$ Torr (b).

cleared by the gap between bunch trains. If the gap is made of 100 buckets (200 ns), then the effect from the residual ions can be neglected. The luminosity reductions with a clearing gap are 20% and 100% for $P_{\mathrm{CO}}=10^{-9}$ and 10^{-8} Torr, respectively. Good vacuum is important to keeping the design luminosity.

Figure 9 shows the tune spread due to the ion distribution. The smear does not work for a small amplitude of less than σ_y. When the amplitude reaches $\sim\sigma_y$, the coherent motion may be smeared, since the growth is reduced, as shown in Fig. 8. This leads to a pulsation of the amplitude growth.

In a worse vacuum, for example, $P_{\mathrm{CO}}=10^{-7}$ Torr, the coherent amplitude of the beam was not saturated at $\sim\sigma_y$. Since the ion distribution blewup at the tail of the train, the beam amplitude grew over σ_y in the same way as in the trapping case.

We discuss the case of the mixture of more species of ions briefly. Each species of ions has a proper frequency (ω_i) given by Eq. (10) in the beam potential. In the scope of linear theory, the superposition rule applies. Simulations including multispecies of ions showed coupled-bunch patterns consistent with the superposition rule.

VI. CONCLUSIONS

Simulations based on a weak-strong model were performed for studying two types of two-beam instabilities due

to ions. Concerning the ion-trapping instability, growth times for various vacuum pressures and stored currents were obtained by using parameters of PF. The growth time was about 1200 turn at $P_{CO}=10^{-9}$ Torr and $I=40$ mA. It was consistent with experiments at the PF. In these conditions, the two-beam instability has been observed and has been cured by exciting octupole magnets with a Landau damping of ~ 1000 turn. Blowup and diffusion of ions were obtained at the vertical beam amplitude of $\sim \sigma_y$ by the simulations. It can explain the pulsation of the instability.

Concerning the fast-ion instability, growth times of each bunch in the train were obtained in the example of KEKB. The growth time was 100 turns at $P_{CO}=10^{-9}$ Torr for a 500 bunch train. Since the rate is near the limit for curing, a vacuum pressure of $P_{CO}=10^{-9}$ Torr is required for KEKB. It was consistent with results from the strong-strong model [9], and was performed using much smaller computer resources.

The instability has usually been cured by a feedback system or by Landau damping. In recent low-emittance rings, a bunch by bunch feedback system was used for such purposes because rapid Landau damping cannot be expected with a small beam size. Since the dynamics of the ion-beam system is affected by the feedback, it may be not clear whether the comparison between the growth and damping rates has any relevance. It may be necessary to perform simulations which include the feedback system.

This method is also available for beam-photoelectron interactions [10,11]. Regarding the beam-photoelectron issue, the linearity of the wake is usually satisfied. However, the linearity is broken in some cases [12]. The present method, which does not require linearity of the wake, can be used to solve such nonlinear wake effects.

ACKNOWLEDGMENTS

The author has discussed the ion-trapping phenomena with S. Sakanaka. Discussions with K. Hirata, S. Kamada, K. Oide, and K. Yokoya were very helpful. This work is based on many studies for ion trapping performed in the KEK Photon Factory. The author acknowledges their contributions. The author also thanks E. Forest for reading the manuscript.

[1] K. Ohmi, K. Hirata, and N. Toge, KEK Report No. 96-73, 1996 (unpublished).

[2] H. Kobayakawa *et al.*, Nucl. Instrum. Methods Phys. Res. A **248**, 565 (1986); S. Sakanaka, M. Izawa, H. Kobayakawa, and M. Kobayashi, Nucl. Instrum. Methods Phys. Res. A **256**, 184 (1987).

[3] E. Keil and B. Zotter, CERN-ISR-TH/71-58, 1971 (unpublished).

[4] H.G. Hereward, CERN 71-15, 1971 (unpublished).

[5] D.G. Koshkarev and P.R. Zenkevich, Part. Accel. **3**, 1 (1972); D. Sagan and A. Temnykh, Nucl. Instrum. Methods Phys. Res. A **344**, 459 (1994).

[6] T.O. Raubenheimer and F. Zimmermann, Phys. Rev. E **52**, 5487 (1995).

[7] G.V. Stupakov, T.O. Raubenheimer, and F. Zimmermann, Phys. Rev. E **52**, 5499 (1995).

[8] M. Bassetti and G. Erskine, CERN ISR TH/80-06, 1980 (unpublished).

[9] K. Yokoya (private communications); KEKB B-Factory Design Report No. 95-7, 1995 (unpublished), pp. 5–17.

[10] M. Izawa, Y. Sato, and T. Toyomasu, Phys. Rev. Lett. **74**, 5044 (1995).

[11] K. Ohmi, Phys. Rev. Lett. **75**, 1526 (1995).

[12] C. Zhang and K. Ohmi, KEK Report No. 96-101, 1996 (unpublished).